Multi-parameters Optimization and Nonlinearity Analysis of the Grating Eddy Current Displacement Sensor

Hongli Qi, Hui Zhao, Weiwen Liu
Department of Instrument Science & Engineering
Shanghai Jiao tong University
Shanghai, China
huizhao@sjtu.edu.cn

***Abstract*—The grating eddy current displacement sensor (GECDS) for displacement or position measurement used in watertight electronic digital caliper was described. The parameters optimization of the sensor is essential for economic and efficient production. The purpose of this study is to determine the optimal combination of the sensor parameters and analyze the effects of these parameters on the nonlinearity of the sensor. The effects of the sensor parameters on nonlinearity are studied by finite element method (FEM). Multi parameter optimization is realized through orthogonal experimental design (OED) method combined with FEM.**

Keywords—grating eddy current displacement sensor, multi parameter optimization, nonlinearity, orthogonal experimental design, finite element method

I. INTRODUCTION

In order to solve the contradiction between long range and high accuracy in displacement or position measurement, grating structure has been used in many sensors, such as optical sensor, capacitive sensor, magnetic sensor and inductive transducer [1-4]. Among these sensors, grating optical sensor and grating capacitive sensor are sensitive to contaminations caused by water, oil and other fluid, grating magnetic sensor is affected by ferromagnetic particles easily. So the three sensors must be sealed or encapsulated to prohibit contaminations from diminishing their effectiveness in hard industry conditions. Compared to the former three sensors, grating inductive sensor is not only insensitive to contaminations caused by fluids, but to dust and ferromagnetic particles. So grating inductive sensor has been widely used in watertight electronic caliper now [4, 5]. However the exciting coil and pickup coil of grating inductive sensor are detached and the shape of pickup coil is relatively complex, which will increase manufacturing and installation costs of the sensor.

According to present situation of grating displacement sensor, we present a new grating displacement sensor based on eddy current effect [6, 7]. The grating eddy current displacement sensor (GECDS) has the function of resistant to liquid, dust and ferromagnetic particles as inductive sensor, which can be used in watertight electronic caliper to realize long range displacement or position measurement with high accuracy in hard industry conditions. The GECDS is different from traditional eddy currents displacement sensors in two main ways. Firstly, the structure of the sensor adopts the form that exciting coil and pickup coil is the same coil, which is different from that the two are detached presented in most previous documents [8-10]. Secondly, the measurement of displacement relies on repetitive inductance variation of coils caused by the change of coupling areas between moving coils and static reflectors.

It is necessary to study the influence of parameters on the characteristics of the sensor to obtain the final desired sensor. The influence of parameters on inductance variation of the GECDS coils is studied qualitatively by means of experiments and finite element method (FEM) [11], other output characteristics of the sensor hasn't been studied now. Because measurement accuracy of sensor is affected by inherent systematic errors, such as the nonlinearity error of the sensor output [12], so the main objective of this paper is to investigate the influence of parameters on nonlinearity of the sensor and realize multi parameters optimization to improve the sensor quality. In this paper, we use finite element method to set up the computer model of the GECDS and use this model to analyze the effects of the sensor's parameters on nonlinearity quantified. Based on nonlinearity analysis of the sensor, multi-parameter optimization method is studied by orthogonal experimental design (OED) combined with finite element analysis.

II. THE PRINCIPLE OF THE GECDS

Fig.1 shows the schematic representation of the GECDS. The sensor consists of a number of coils and reflectors mostly. Reflectors are located on the stator scale with a fixed pitch λ repetitively. Coils are located on the moving scale (invisible in fig.1) and move transversely with moving scale. Coils and reflectors are all made of copper conductor, which is nonmagnetic. When alternating current with high frequency pass through coils which move transversely, coupling areas between coils and reflectors will be changed, magnetic flux within coils will be changed accordingly, which will result in inductance variation of coils. So the displacement between coils and reflectors S could be converted into inductance

978-1-4244-1676-9/08 /$25.00 ©2008 IEEE

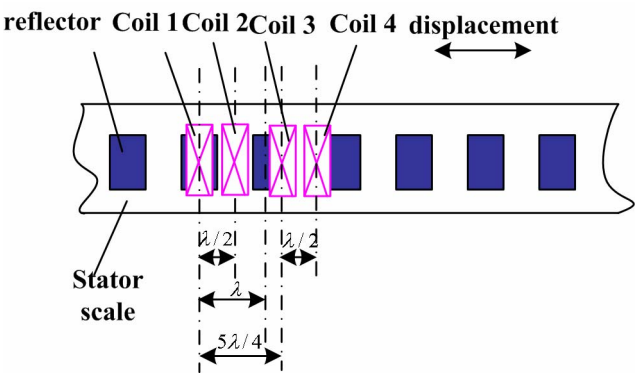

Figure 1. Schematic diagram of the principle of the sensor

variation of coils. Inductance value can be sensed by tracking the amplitude of current, voltage or frequency which is dependent on inductance of coils by measurement circuits, so the displacement S can be achieved. In a complete cycle (i.e. the fixed pitch λ), induction of coils vary from minimum to maximum and then to minimum again. Let coils move the displacement S, inductance of coils vary repetitively, the displacement S can be calculated by the following formula, i.e.

$$S = n\lambda + x. \tag{1}$$

Where S denotes the displacement between coils and reflectors, n denotes the numbers of cycle λ and x denotes the little displacement in a cycle λ.

Coil 1 and coil 2, coil 3 and coil 4 are apart from each other by $\lambda/2$ and are connected in differential form respectively to enhance measurement sensitivity and avoid measurement blind areas. Coil 1 and coil 3, coil 2 and coil 4 are apart from each other by $5\lambda/4$ and output sinusoidal and cosine signal separately to measure the little displacement x. Coil 1 and coil 2 output differential frequency signal $f_{12} = f_1 - f_2$, coil 3 and coil 4 output differential frequency signal $f_{34} = f_3 - f_4$. Since coil 1 and 3, coil 2 and 4 are apart from each other by $5\lambda/4$ respectively, waveforms of differential frequency against displacement are shifted in phase for $\lambda/4$. Fig.2 shows the frequency variation of coil 1 and 2 against the displacement which is equal to the length of two pitches (i.e. 10mm). The frequency differences are shown in Fig.3. The two figs indicated that $\lambda/2$ segments of the differential frequency f_{12} have a better sensitivity in MHz/mm than corresponding segments of the original coils and eliminates the blind areas of wave valley.

Because the differential frequency curve f_{12} approaches to curve f_{34} approaches to the sinusoidal curve approximately, curves f_{12} and f_{34} can be expressed by following formulas approximately, i.e.

$$f_{12} = A\cos\left(\frac{2\pi}{\lambda}x\right), \tag{2}$$

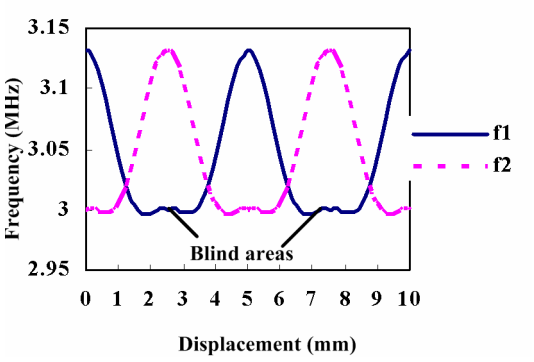

Figure 2. Frequency waveforms of coil 1 and 2

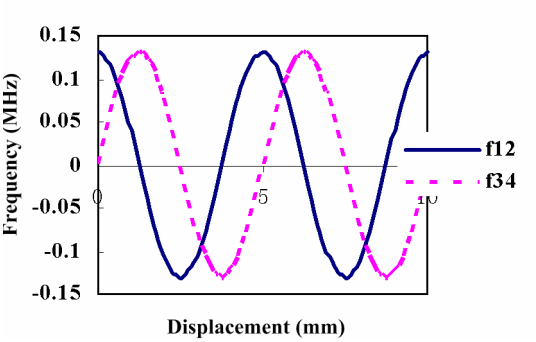

Figure 3. Differential frequency waveforms

$$f_{34} = A\sin\left(\frac{2\pi}{\lambda}x\right). \tag{3}$$

Let the phase angle be

$$\varphi = \frac{2\pi}{\lambda}\cdot x, \tag{4}$$

$$\varphi = \arctan\left(\frac{f_{34}}{f_{12}}\right) = \arctan\left[\frac{\sin(\frac{2\pi}{\lambda}\cdot x)}{\cos(\frac{2\pi}{\lambda}\cdot x)}\right]. \tag{5}$$

Fig.4 illustrates the linear variation of the phase angle φ against the displacement which is equal to the length of two pitches according to the formula 5. It can be seen that the

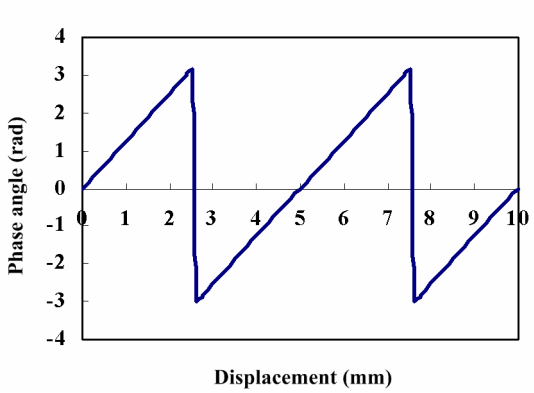

Figure 4. The linear variation of angle phase against displacement

phase angle is proportional to the displacement in a complete cycle, so the little displacement x can be obtained through phase angle φ, i.e.

$$x = \frac{\lambda\varphi}{2\pi}. \tag{6}$$

Assuming n (numbers of cycle λ) has been acquired, the displacement S can be calculated by (1).

III. SETTING UP THE MODEL

We used electromagnetic field finite element software Maxwell 3D simulator [13] to set up the computer model of the GECDS in this study. Due to the highest inductance density of spiral coil configuration comparative to planar coil [14], multi-layer planar rectangular spiral coils has been selected for our work. The sensor was designed as a 10-layer of planar spiral coils and successive layers are connected via contact. A schematic representation of the sensor with multi-layer coils is presented in Fig.5, where the structure was simplified to a stack of only 2-layer of planar spiral coils.

When setting up the computer model of the sensor, it's necessary to make all parameters of the model approaching to real parameters of the sensor to make simulation results agree well with experimental results in quantity. In this study, the real numbers of layer is 10. It's could be excessively time-consuming if we set up model according to the real situation. So the sensor model with 2-layer coils was used in this paper. Induction variation of 2-layer coils can be obtained through simulation. The relationship between induction and the numbers of layer can be achieved through deduction, and

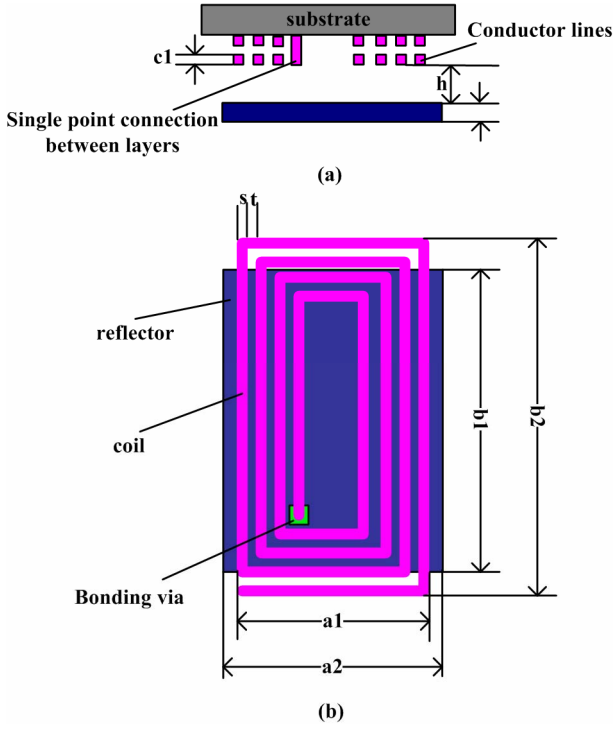

Figure 5. Schematic presentation of multi-layers coils

then induction variation of 10-layer coils can be acquired finally. When all other parameters of rectangular coils with rectangular cross-section are invariant, induction L is proportional to the square of the turns of the coil [15, 16]. So induction of 10-layer coils can be obtained through the following expression, i.e.

$$L_{10} = (\frac{10}{2})^2 \cdot L_2 = 25L_2. \tag{7}$$

Where L_{10} denotes the inductance of 10-layer coil and L_2 denotes the inductance of 2-layer coil. As frequency modulation circuit was used in this study, frequency variation of simulation results could be obtained according to the following equation

$$f = \frac{1}{2\pi\sqrt{LC}}. \tag{8}$$

The capacitance C is equal to the value of real measurement circuit.

IV. NONLINEARITY ANALYSIS OF THE SENSOR

The main objective of this paper is to investigate the influence of parameters on nonlinearity of the GECDS sensor. The nonlinearity error curve in a complete cycle λ was shown in fig. 6, which indicated the error variation rule in one cycle. According to our experience in experiments and simulation, nonlinearity error of the sensor was affected by many parameters of the sensor and the sensor has different maximum nonlinearity error in one cycle for different parameters.

Since geometric parameters of coils are complex comparative to that of reflectors, as shown in fig. 5, simulation were implemented through changing reflectors' parameters of the model in this study.

At given parameters of coils, the simulation results shown that the main parameters affecting nonlinearity error were: reflector length, reflector width and the axial gap between coils and reflectors. The effects of altering reflector length, reflector width and axial gap on nonlinearity were summarized in fig.7,

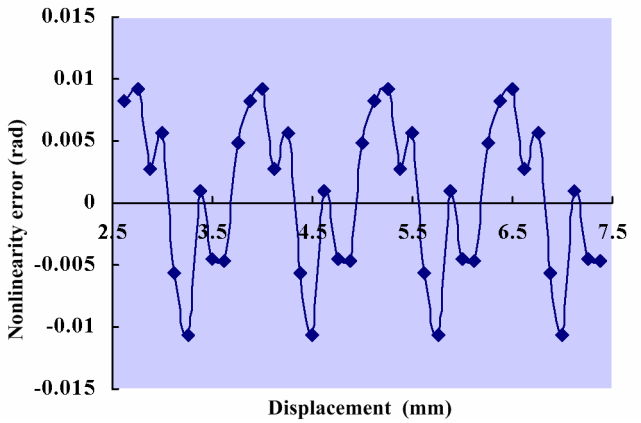

Figure 6. Nonlinearity error variation in a cycle

fig.8 and fig.9. These figs indicated that nonlinearity error variation curves were similar with parabolas when altering a certain parameter; nonlinearity error would arrive to minimum at some point of the parabola, which correspond to a certain parameter value; increasing or decreasing of parameter value would both increase nonlinearity error of the sensor.

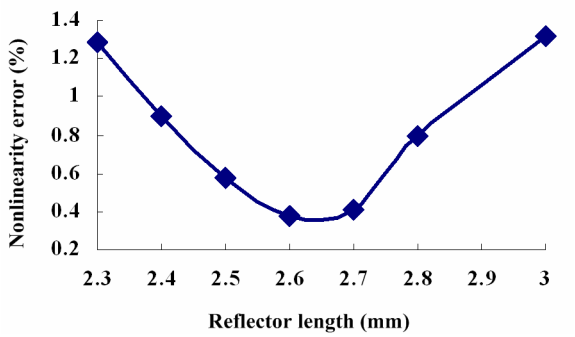

Figure 7. Effect of reflector length on nonlinearity

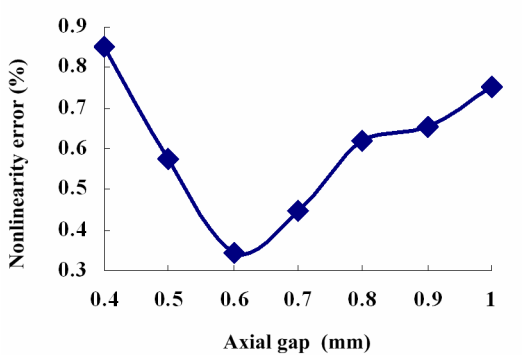

Figure 8. Effect of axial gap on nonlinearity

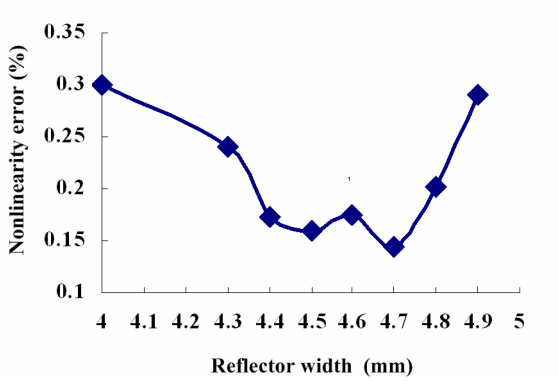

Figure 9. Effect of reflector width on nonlinearity

The nonlinearity error curve in fig.7 was obtained at the axial gap of 0.5mm and the reflector width of 4mm, which shown nonlinearity error arrived minimum 0.38% approximately when the reflector length was 2.6mm. Let the reflector length be 2.6mm, we could get the error curve shown in fig.8 by changing axial gap at given reflector width of 4mm. It can be seen that the minimum nonlinearity error was 0.34% when axial gap was 0.6mm. The error curve in fig.9 was obtained by altering reflector width at the reflector length 2.6mm and axial gap 0.6mm. To sum up, nonlinearity error could arrive minimum 0.14% at reflector length 2.6, axial gap 0.6mm and reflector length 4.7mm.

The above nonlinearity analysis which used exhaustive algorithm revealed the variation rules of nonlinearity error when altering parameters value. The exhaustive algorithm is time consuming extremely. Moreover the interaction among parameters was considered in the algorithm, since each optimized result, such as minimum nonlinearity error (0.38%) was obtained based on that the other two parameters were fixed. So the minimum nonlinearity error (0.14%) just is near optimal.

In order to reduce computer time and improve production efficiency, a multi-parameters optimization method was presented in the next section to obtain optimum.

V. MULTI-PARAMETER OPTIMIZATION DESIGN OF THE GECDS

The main objective of this paper is to investigate the influence of parameters on nonlinearity and realize multi-parameters optimization of the sensor. In this section, we presented a method to achieve the above target by combining finite element analysis and the OED method.

The OED method is an experimental design method which has been applied in a wide range of industries [17-19]. It adopts a set of orthogonal arrays to analyze the effect of parameters on specific quality characteristics. These arrays use a small number experiment but get maximum information. The basic steps are as follows: First, the quality characteristics and the parameters are selected, and then the appropriate orthogonal array is constructed. The finite element simulation is performed based on the arrangement of the orthogonal array. Analysis of simulation results is performed to see which parameters are significant factors.

As mentioned above, the main parameters affecting nonlinearity error were: reflector length, reflector width and the axial gap between coils and reflectors. The objective function of nonlinearity error is defined by following expression, i.e.

$$E_i = f(a_i, b_i, h_i)\,. \tag{9}$$

Where E_i denotes nonlinearity error, a_i, b_i and h_i denotes the reflector length, the reflector width and the axial gap separately. Our purpose is to obtain the minimum nonlinearity error when the sensor has the optimal parameters combined.

The three parameters to be evaluated in this study are shown in Table 1. To evaluate these factors (parameters), three levels were chosen for each parameter according to the above analysis results of nonlinearity error. For three factors with three levels for each parameter, experimental layout of an L_9 orthogonal array was selected for present research. Table 2 shows the L_9 orthogonal array in which the 9 times experiments are carried out to investigate the effects of the three factors on nonlinearity.

The simulation parameters and nonlinearity error of the 9 times experiments are shown in table 2. The table indicated the

TABLE I. LEVEL OF PARAMETERS

Desig-nation	Parameters (mm)	Level 1	Level 2	Level 3
a	Reflector length	2.5	2.6	2.7
b	Reflector width	4.6	4.7	4.8
h	Axial gap	0.5	0.6	0.7

TABLE II. EXPERIMENTAL LAYOUT USING ORTHOGONAL ARRAY

Experimental No.	Parameters (mm)			Nonlinearity Error (%)
	a	*h*	*b*	
1	1(2.5)	1(0.5)	1(4.6)	0.6
2	1(2.5)	2(0.6)	2(4.7)	0.36
3	1(2.5)	3(0.7)	3(4.8)	0.29
4	2(2.6)	1(0.5)	2(4.7)	0.34
5	2(2.6)	2(0.6)	3(4.8)	0.2
6	2(2.6)	3(0.7)	1(4.6)	0.17
7	3(2.7)	1(0.5)	3(4.8)	0.22
8	3(2.7)	2(0.6)	1(4.6)	0.37
9	3(2.7)	3(0.7)	2(4.7)	0.51

TABLE III. AVERAGE NONLINEARITY ERROR FOR EACH PARAMETER

Desig-nation	Average nonlinearity error (%)			Level difference
	Level 1	Level 2	Level 3	
a	0.42	0.24	0.37	0.18
b	0.38	0.4	0.24	0.16
h	0.39	0.31	0.32	0.08

nonlinearity error arrived minimum (0.17%) at reflector length of 2.6mm, axial gap of 0.7mm and reflector width 4.6mm. It can be seen that the optimized results of OED method were different from but close to that of exhaustive algorithm. The cause was that OED method was based on the assumption that all parameters were irrelevant completely, i.e. disregarding interaction among parameters. But the interaction among parameters was considered in exhaustive algorithm. Though the results of OED method were different from that of exhaustive algorithm slightly, it could instruct experiment for multi parameter optimization.

The average nonlinearity error for each parameter at level 1 to 3 is shown in table 3. Level difference shown in table 3 is equal to the maximum average nonlinearity error subtract minimum average nonlinearity error of each level. The significant degree of effect on nonlinearity of three parameters could be obtained by level difference value. The larger level difference value is, the more influence of the parameter on nonlinearity is. We could get conclusions as follows: the significant parameters influencing nonlinearity error were reflector length and reflector width; the effect of axial gap was small compared to that of reflector length and reflector width.

VI. CONCLUSIONS

This paper presented the GECDS for displacement or position measurement. To optimize sensor parameters, the sensor's computer model has been set up by FEM method. In this paper, a new method has been used to analyze the effect of parameters on nonlinearity and realize the multi- parameters optimization by combining finite element analysis and the OED method. From the results, some conclusions can be drawn as follows: the significant parameters affecting the nonlinearity can be identified by OED method; reflector length and reflector width have the greatest effects on nonlinearity of the sensor compared axial gap; the corresponding optimal parameters can be obtained when nonlinearity error arrives minimum. It can be seen that it's effective combining FEM and OED method.

REFERENCES

[1] Christine Prelle, Frédéric Lamarque, and Philippe Revel, "Reflective optical sensor for long-range and high-resolution displacements," Sensors and Actuators, vol. A127, pp. 139-146, 2006.

[2] Neal A. Hall, Wook Lee, Jared Dervan, and F. Levent Degertekin, "Micromachined capacitive transducer with improved optical detection for ultrasound applications in air," IEEE Ultrasonics Symp. pp. 1027-1030, 2002.

[3] I.I. Davidenko, A.J.Al-Kadhimi, "Magnetic grating in garnets in spatially periodic effective and real magnetic field," J. Magnetism and Magnetic Materials 272-276, pp. 363-364, 2004.

[4] Mitutoyo Corporation, Induced current absolute position transducer using a code-track-type scale and read head: US patent, 08/790,494. 1998-11-24.

[5] Mitutoyo Corporation, Electronic caliper using a reduced offset induced current position transducer, US patent, 09/527,518, 2002-1-1.

[6] Zhao Hui, Ma Dong li, Liu Weiwen and Yu Pu, "Design of a new inductive grating displacement sensor and application in liquid resistant caliper", Journal of Shanghai Jiaotong University, vol. 38 (8), pp. 1382-1384, 2004.

[7] Zhao Hui, Liu Weiwen, Yu Pu and Tao wei, "Summary on water-proof electronic digital caliper," New Technology & New Process (12), pp. 7-10, 2002.

[8] D. Kacprzak, T. Taniguchi, K. Nakamura, S. Yamada and M. Iwahara, Novel eddy current testing sensor for the inspection of printed circuit boards, IEEE Transactions on magnetic 37 (4) (2001) 2010-2012.

[9] Dragan Dinulovic and Hans H.Gatzen, Microfabricated inductive micropositioning sensor for measurement of a linear movement, IEEE Sensors Journal 6 (6) (2006) 1482-1487.

[10] S. Yamada, K. Chomsuwan, Y. Fukuda, M. Iwahara, H. Wakiwaka and S.Shoji, Eddy-current testing probe with spin-valve type GMR sensor for Printed Circuit Board Inspection, IEEE Transactions on Magnetics, 40 (4) (2004) 2676-2678.

[11] Zhou Danli, Zhao Hui, Liu Weiwen and Hong Haitao, "3-D FEA simulating study on the parameters of eddy current displacement sensor," Computer Measurement & Contron, Vol. 13(6), pp.618-620, 2005.

[12] Shizhou Zhang, Satoshi Kiyono, "An absolute calibration method for displacement sensors," Measurement, Vol. 29, pp. 11-20, 2001.

[13] Ansoft Maxwell 3D Field Simulator v11 User's Guide: Ansoft Corp

[14] Yukio Hamasaki, Takahiro Ide, Fabrication of Multi-layer eddy current micro sensors for non-destructive inspection of small diameter pipes, in: Micro Electro Mechanical Systems, Proceedings. IEEE, 1995, 232-237.

[15] R.J. Ditchburn, S.K. Burke, Planar rectangular spiral coils in eddy-current non-destructive inspection , NDT&E International 38 (2005) 690–700.

[16] Theodoulidis TP, Kriezis EE, Impedance evaluation of rectangular coils for eddy current testing of planar media, NDT&E International 35 (2002) 407–414.

[17] Deyun Chen, Mouzun Li, and Wang Lili, "Parameters Optimization and simulation of transducer based on finite element method in electrical capacitance tomography system," IEEE Proc. IMSCCS, 2006.

[18] Avanish Kumar Dubey.Vinod Yadava, "Robust parameter design and multi-objective optimization of laser beam cutting for aluminium alloy sheet," Int J Adv Manuf Technol, 2007.

[19] Bing Li. T.J. Nye. Don R. Metzger, "Multi-objective optimization of forming parameters for tube hydroforming process based on the Taguchi method," Int J Adv Manuf Technol, Vol. 28, pp.23-30, 2006.